J|A|C|S
ARTICLES
Published on Web 09/19/2006

Supramolecular Nanopatterns Self-Assembled by Adenine−Thymine Quartets at the Liquid/Solid Interface

Wael Mamdouh, Mingdong Dong, Sailong Xu, Eva Rauls, and Flemming Besenbacher*

Contribution from the Interdisciplinary Nanoscience Center (iNANO) and Department of Physics and Astronomy, University of Aarhus, DK-8000 Aarhus C, Denmark

Received July 13, 2006; E-mail: fbe@inano.dk

Abstract: By means of scanning tunneling microscopy (STM), we have observed for the first time well-ordered supramolecular nanopatterns formed by mixing two complementary DNA bases: adenine (A) and thymine (T), respectively, at the liquid/solid interface. By mixing A and T at a specific mixing molar ratio, cyclic structures that were distinctly different from the structures observed by the individual base molecules separately were formed. From an interplay between the STM findings and self-consistent charge density-functional based tight-binding (SCC-DFTB) calculation method, we suggest formation of A−T−A−T quartets constructed on the basis of A−T base pairing. The formation of the A−T−A−T quartets opens new avenues to use DNA base pairing as a way to form nanoscale surface architecture and biocompatible patterned surfaces particularly via host−guest complexation that might be suitable for drug design, where the target can be trapped inside the cavities of the molecular containers.

1. Introduction

Self-assembly of molecular building blocks is a very interesting route for building nanostructures and nanodevices with high precision on the nanometer scale.[1,2] Self-assembly is a natural phenomenon that can be observed in many biological, chemical, and physical processes. The motivation and inspiration to continue exploring self-assembly are obvious when studying the most advanced biological system known: the living cell.[3] This unimaginably complex machinery made of organic molecules and polymers is formed and operates by self-assembly to a large degree.

The precision and efficiency of this self-assembly process derive from specific molecular interactions between proteins, DNA, RNA, and other compounds including lipids, carbohydrates, and so forth. DNA is in particular an essential building block for life and thus plays a pivotal role in cell biology. In addition, DNA is a unique biomolecule suitable for the design and formation of artificial nanostructures by self-assembly since it is possible to use base sequences to encode instructions for assembly in a predetermined fashion at the nanometer scale.[4] In nature, complementary DNA bases interact with each other via intermolecular hydrogen bonding, leading to the formation of the fascinating DNA double helices.[5]

In the double helical DNA structure, complementary base pairing via hydrogen bonds in DNA is of utmost importance,[6] and the exquisite specificity of DNA complementary base pairing allows a large set of nucleotide sequences to be used for the design of binding interactions. Although the structural differences between nucleic acid bases are small, the differences in their chemistry and electronic properties are significant.[7]

It is a great challenge for the future to understand the mechanisms behind the assembly of DNA bases and their complexation with proteins and amino acids and with more complex biological systems, which may lead to the formation of supramolecular complexes and nanoscale structures. It is therefore of great importance to study self-assemblies of nucleic acid base molecules as a means to explore their inter- and intramolecular hydrogen bonding properties. A variety of supramolecular structures formed by nucleic acid bases can be formed by changing the experimental conditions. Therefore, in the past the adsorption of nucleic acid base molecules has been extensively studied theoretically and experimentally.[8−11] However, thorough and detailed studies of complementary DNA base pairing on surfaces are rather scarce.

Scanning probe microscopy (SPM) has proven to give new detailed atomic-scale insight into the self-assembly and dynam-

(1) De Feyter, S.; De Schryver, F. C. *Chem. Soc. Rev.* **2003**, *32*, 139−150.
(2) (a) Seto, C. T.; Whitesides, G. M. *J. Am. Chem. Soc.* **1991**, *113*, 712−713. (b) Bowden, N.; Terfort, A.; Carbeck, J.; Whitesides, G. M. *Science* **1997**, *276*, 233−235. (c) Whitesides, G. M.; Mathias, J. P.; Seto, C. T. *Science* **1991**, *254*, 1312−1319.
(3) Alberts, B.; Johnson, A.; Lewis, J.; Raff, M.; Roberts, K.; Walter, P. *Molecular Biology of the Cell*, 4th ed.; Garland Science-Taylor & Francis Group: New York, 2002.
(4) (a) Gothelf, K. V.; LaBean, T. H. *Org. Biomol. Chem.* **2005**, *3*, 4023−4037. (b) Yan, H.; Park, S. H.; Finkelstein, G.; Reif, J. H.; LaBean, T. H. *Science* **2003**, *301*, 1882−1884. (c) Mao, C. D.; LaBean, T. H.; Reif, J. H.; Seeman, N. C. *Nature* **2000**. (d) Yan, H.; Feng, L. P.; LaBean, T. H.; Reif, J. H. *J. Am. Chem. Soc.* **2003**, *125*, 14246−14247.
(5) (a) Watson, J. D.; Crick, F. C. H. *Nature* **1953**, *171*, 737−738. (b) Crick, F. H. C.; Watson, J. D. *Proc. R. Soc. London, Ser. A* **1954**, *223*, 80−96.
(6) Saenger, W. *Principles of Nucleic Acid Structure*; Springer, Berlin, 1984.
(7) Tao, N. J.; DeRose, J. A.; Lindsay, S. M. *J. Phys. Chem.* **1993**, *97*, 910−919.
(8) (a) Kelly, R. E. A.; Kantorovich, L. N. *Surf. Sci.* **2005**, *589*, 139−152. (b) Kelly, R. E. A.; Kantorovich, L. N. *J. Phys. Chem.* **2006**, *110*, 2249−2255. (c) Kelly, R. E. A.; Lee, Y. J.; Kantorovich, L. N. *J. Phys. Chem. B* **2005**, *109*, 22045−22052.

ics of organic and biomolecular adsorbates on various substrates.[1] In the present context, the unique ability of SPMs to directly observe individual DNA bases will allow novel insights into how DNA bases interact with each other to form functional nanoscale assemblies.[12]

In this work, we have investigated the self-assembly of two DNA bases, A and T, respectively, and also how their mixture will self-assemble at the liquid−solid interface by STM. In control experiments, where the individual bases are adsorbed separately at the graphite surface, dimer formation is found to dominate, and domains containing molecular networks constructed by A and T dimers, respectively, are observed. Interestingly, after mixing the two complementary bases, new cyclic structures that are significantly different from the structures obtained by the pure DNA base molecules in the control experiments are observed. The new mixed A+T structures appear in the STM images as cyclic structures (doughnuts) separated by single chains. To gain further insight into the nature and composition of these cyclic and chain structures, self-consistent charge density-functional based tight-binding (SCC-DFTB) calculations were performed, and the results are discussed in detail and compared to the experimental STM findings in the following sections.

2. Experimental and Computational Section

The STM experiments were performed at the liquid/solid interface under ambient conditions at room temperature using a MultiMode SPM system with a Nanoscope IIIa controller (Veeco Instruments Inc., Santa Barbara, CA). STM tips were mechanically cut from a 0.25-mm Pt/Ir (80/20) wire and tested on freshly cleaved highly oriented pyrolytic graphite (HOPG) surfaces (HOPG, grades ZYA and ZYB, Advanced Ceramics Inc., Cleveland, OH and NT-MDT, respectively). Prior to imaging, adenine and thymine were dissolved in 1-octanol (Aldrich 99%) at a concentration of 2 mg/1 g for adenine (A) and 0.8 mg/1 g for thymine (T), respectively, and a drop of each solution was applied separately onto a freshly cleaved surface of HOPG. The STM tip was immersed in the solution, and images were recorded at the 1-octanol/graphite interface. The (A+T) mixture was prepared by mixing a solution of adenine dissolved in 1-octanol with a solution of thymine dissolved in 1-octanol, and one drop of the A+T mixture was applied onto a freshly cleaved HOPG surface. Several mixing molar ratios have been prepared and imaged by STM, and in each case, a high degree of dynamic was observed upon adsorption of a drop of the A+T mixed solution onto the HOPG surface, which hindered the formation of well-ordered patterns. However, well-ordered supramolecular structures observed in the high-resolution STM images presented in this work have only been obtained at a significantly high mixing molar ratio (350A:1T). On the other hand, the other mixing molar ratios showed domains that only contain the pure bases (phase separation) and some cyclic structures, to a minor extent, that were disordered on the surface (data not shown). The high mobility of these cyclic structures on the substrate hindered their long-term stability on the time scale of the experiments.

Several tips and HOPG samples were used to ensure reproducibility and to avoid artifacts. The STM images were obtained in the constant height mode. For calibration purposes, recording of the STM images of the A, T, and A+T mixture was followed by imaging the graphite substrate underneath under the same experimental conditions, except for the lowered bias voltage. Image analysis was performed via Scanning Probe Image Processor (SPIP) software (Image Metrology ApS, Lyngby, Denmark),[13] and the images were corrected for any drift using the recorded graphite images for calibration purposes, which allowed us to determine the unit cells more accurately. Furthermore, the correlation averaging method[13,14] was used for the more detailed image analysis and for the display of the high-resolution STM images. We always investigated very thoroughly that this did not affect the unit cell parameters. The imaging parameters, tunneling current (I_{tunn}), and sample bias (V_{bias}), are stated in the figure captions.

Theoretical simulations were performed within the framework of the SCC-DFTB method.[15] All involved atoms were fully relaxed without constraints. Due to the large number of atoms, in our calculations we have included neither the solvent molecules nor the substrate. This approach has already been applied successfully to explain the molecular structures formed by the other two complementary DNA bases: guanine and cytosine.[12]

3. Results and Discussion

In Figure 1, high-resolution STM images of physisorbed adlayers of adenine (Figure 1A) and thymine (Figure 1B) at the 1-octanol/graphite interface are shown. In the high-resolution STM image of the A adlayer, every bright spot is related to one A molecule. It is observed that every two A molecules are packed as A−A dimers (indicated with yellow bars) stabilized via hydrogen bonding. These A−A dimers lead to the formation of a stable two-dimensional A network. The unit cell indicated in Figure 1A,C contains four A molecules. The intermolecular distances between two adjacent A−A dimers are determined to be $a = 0.8 \pm 0.1$ nm, $b = 2.2 \pm 0.2$ nm, and $\gamma = 76 \pm 2.3°$ (Table 1). The orientation of the A−A dimers along unit cell vector *b* is altered from one row to another, leading to "zigzag" chains along unit cell vector *b* observed in Figure 1A,C. Upon adsorption of A−A dimers on the substrate, it is possible to obtain both homochiral and heterochiral molecular networks (see Supporting Information SP1). In Figure 1C, the calculated model for the heterochiral molecular network constructed by A−A dimer is depicted, and the model is seen to be in good agreement with both the heterochiral molecular network observed in the STM image in Figure 1A as well as with many structural models reported earlier by other groups.[16]

Figure 1B shows a high-resolution STM image of physisorbed T molecules at the 1-octanol/graphite interface. A high degree of diffusion dynamic is observed upon adsorption of T molecules

(9) (a) Kelly, R. E. A.; Lee, Y. J.; Kantorovich, L. N. *J. Phys. Chem. B* **2005**, *109*, 11933−11939. (b) Tanaka, H.; Kawai, T. *Jpn. J. Appl. Phys.* **1996**, *35*, 3759−3763 (Part 1, No. 6B). (c) Furukawa, M.; Tanaka, H.; Kawai, T. *Surf. Sci.* **1997**, *392*, L33−L39. (d) Tanaka, H.; Yoshinobu, J.; Kawai, M.; Kawai, T. *Jpn. J. Appl. Phys.* **1996**, *35*, L244−L246 (Part 2, No. 2B). (e) Nakagawa, T.; Tanaka, H.; Kawai, T. *Surf. Sci.* **1997**, *770*, L144−L148. (f) Freund, J. E.; Edelwirth, M.; Krobel, P.; Heckl, W. M. *Phys. Rev. B* **1997**, *55*, 5394−5397. (g) Heckl, W. M.; Smith, D. P. E.; Binnig, G.; Klagges, H.; Hänsch, T. W.; Maddocks, J. *Proc. Natl. Acad. Sci. U.S.A.* **1991**, *88*, 8003−8005. (h) Allen, M. J.; Balooch, M.; Subbiah, S.; Tenth, R. J.; Siekhaus, W.; Barlhorn, R. *Scanning Microsc.* **1991**, *5*, 625−630.
(10) (a) Tao, N. J.; Shi, Z. *J. Phys. Chem.* **1994**, *98*, 1464−1471. (b) Srinivasan, R.; Murphy, J. C. *Ultramicroscopy* **1992**, *42*−*44*, 453−459. (c) Sowerby, S. J.; Edelwirth, M.; Heckl, W. M. *J. Phys. Chem. B* **1998**, *102*, 5914−5922. (d) Dretschkow, Th.; Dakkouri, A. S.; Wandlowski, Th. *Langmuir* **1997**, *13*, 2843−2856. (e) Sowerby, S. J.; Heckl, W. M.; Petersen, G. B. *J. Mol. Evol.* **1996**, *43*, 419−424. (f) Edelwirth, M.; Freund, J.; Sowerby, S. J.; Heckl, W. M. *Surf. Sci.* **1998**, *417*, 201−209.
(11) Otero, R.; Schöck, M.; Molina, L. M.; Lægsgaard, E.; Stensgaard, I.; Hammer, B.; Besenbacher, F. *Angew. Chem., Int. Ed.* **2005**, *44*, 2270−2275.
(12) Xu S.; Dong, M.; Rauls, E.; Otero, R.; Linderoth, T. R.; Besenbacher, F. *Nano Lett.* **2006**, *6*, 1434−1438.
(13) Image Metrology Web site. http://www.imagemet.com.
(14) Samorí, P.; Engelkamp, H.; de Witte, P.; Rowan, A. E.; Note, R. J. M.; Rabe, J. P. *Angew. Chem.* **2001**, *113*, 2410−2412; *Angew. Chem., Int. Ed.* **2001**, *40*, 2348−2350.
(15) Frauenheim, Th.; Seifert, G.; Elstner, M.; Hajnal, Z.; Jungnickel, G.; Porezag, D.; Suhai, S.; Scholz, R. *Phys. Status Solidi B* **2000**, *217*, 41−62.
(16) (a) Uchihashi, T.; Okada, T. *Phys. Rev. B* **1999**, *60*, 8309−8313. (b) Perdigão, L. M. A.; Staniec, P. A.; Champness, N. R.; Kelly, R. E. A.; Kantorovich, L. N.; Beton, P. H. *Phys. Rev. B* **2006**, *73*, 195423−1−7.

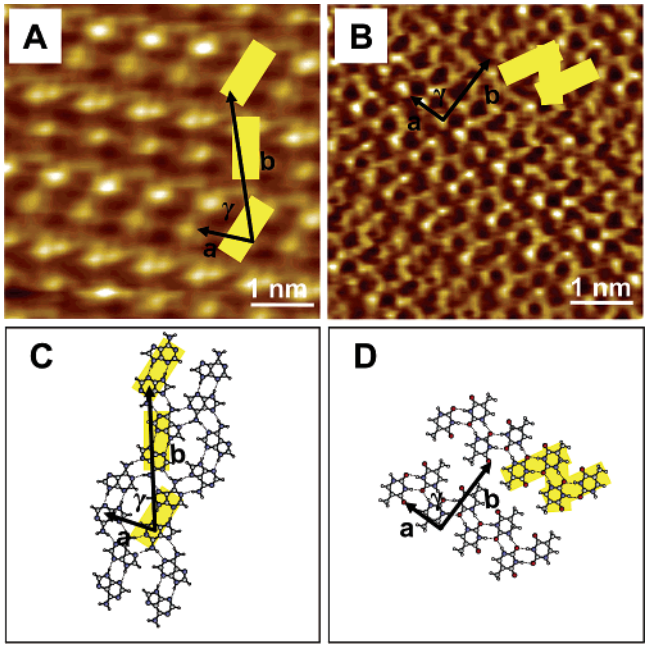

Figure 1. (A) High-resolution correlation-averaged STM images of physisorbed adlayers of adenine (A) and thymine (B) at the 1-octanol/graphite interface. The tunneling parameters are $I_{tunn} = 1.58$ nA, $V_{bias} = -981.6$ mV for adenine and $I_{tunn} = 0.54$ nA, $V_{bias} = -248.0$ mV for thymine, respectively. (C) and (D) Calculated models of an A−A heterochiral network and T−T dimer chains, respectively. Dimers are illustrated with yellow bars. The unit cells are indicated in black.

Table 1. Comparison of the Lattice Parameters Determined for the Observed Different Adlayer Structures as Derived from the Analysis of the STM Images

	a (nm)	*b* (nm)	γ (deg)
pure adenine (A)	0.8 ± 0.1	2.2 ± 0.2	76 ± 2.3
pure thymine (T)	0.8 ± 0.1	1.5 ± 0.2	87 ± 2.5
mixture A+T	1.0 ± 0.2	2.3 ± 0.2	88 ± 2

on the graphite surface. The observed bright rows correspond to T−T dimers aligned into adjacent parallel chains that are stabilized via internal hydrogen bonding as indicated in the calculated model depicted in Figure 1D. Each T molecule is hydrogen-bonded to two of its neighbors in a chainlike structure through four hydrogen bonds, leading to a "zigzag" formation along unit cell vector *a* as indicated with yellow bars in Figure 1B,D, respectively. The unit cell indicated in Figure 1B,D contains two T molecules. The intermolecular distances between two adjacent T−T dimers are determined to be $a = 0.8 \pm 0.1$ nm, $b = 1.5 \pm 0.2$ nm, and $\gamma = 87 \pm 2.5°$ (Table 1). The calculated molecular model formed by the T−T dimers is in good agreement with previously proposed models.[17]

To create supramolecular patterned surfaces based on DNA complementary base pairing between A and T molecules, we mixed solutions of pure A and T bases in 1-octanol together and applied the mixed solution onto the graphite substrate. Figure 2 shows high-resolution STM images of A+T mixture physisorbed at the 1-octanol/graphite interface. Interestingly, a well-ordered molecular pattern, which is significantly different from the structures observed in Figure 1 in the control experiments of the individual pure base molecules, is observed. In

(17) Sowerby, S. J.; Petersen, G. B. *J. Electroanal. Chem.* **1997**, *433*, 85−90.

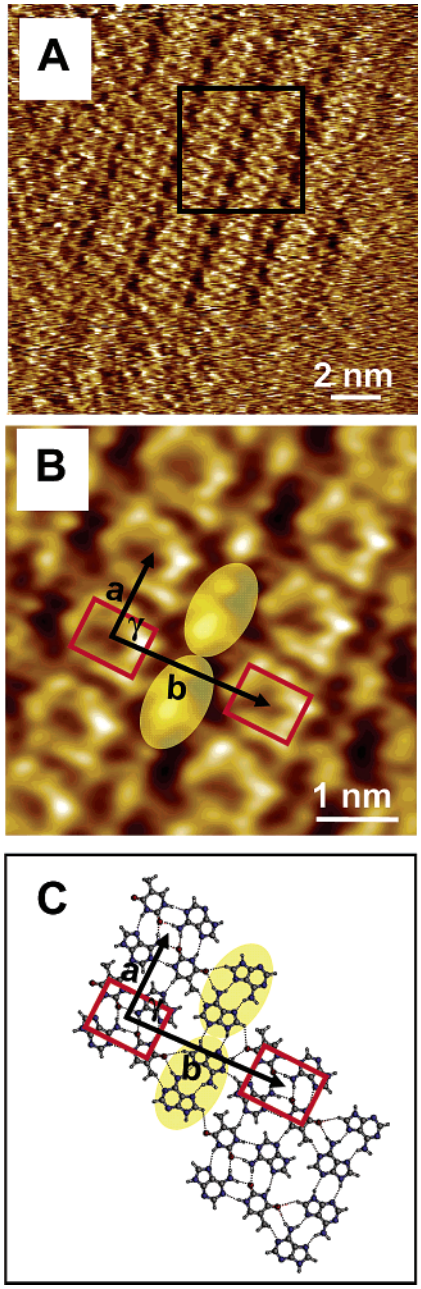

Figure 2. (A) STM image of A+T mixture at the 1-octanol/graphite interface. The tunneling parameters are $I_{tunn} = 1.2$ nA and $V_{bias} = -447.4$ mV. (B) Correlation-averaged zoom-in image of the area indicated in image (A) by a black square. (C) Calculated model suggesting that each cycle is composed of four molecules: 2A+2T, leading to reverse Hoogsteen A−T−A−T quartets adjacent to homochiral chains of A−A dimers. Cycles and A−A dimers are indicated with red rectangles and yellow ovals, respectively. The unit cell is indicated in black.

the observed mixed A+T molecular patterns, two different coexisting features are clearly revealed: (i) rows that contain "cyclic" structures (indicated with red rectangles in Figure 2B,C) and which are separated by (ii) "single chains" that contain only bright spots (indicated with yellow ovals in Figure 2B,C), respectively.

Although the resolution of the STM images of the A+T mixture in Figure 2 is fairly high, we are faced with the inherent problem of STM that the images reflect a fairly detailed convolution of both geometrical and electronic structure. Thus,

we do not know a priori (if based only on the contrast of the STM image) whether a bright spot is related to an A molecule or a T molecule involved in a cyclic or in a single-chain structure, respectively. The situation, however, is even more complicated to distinguish whether a spot is related to the center of a molecule at this site, or only some parts of the molecule (such as methyl groups or maybe most likely here oxygen atoms in T molecules), or, for example, the space between two molecules, where they bind together. Therefore, to gain further insight into the nature and the composition of the cycles and the single chains observed in Figure 2, we have compared the observed STM images with structures obtained from the theoretical SCC-DFTB calculations.

Taking into account the size of each cyclic substructure observed in Figure 2 (0.9 ± 0.2 nm along unit cell vector *a*, and 1.5 ± 0.1 nm along unit cell vector *b*), it is obvious that the cyclic substructures are constructed by more than two and maybe by even three to four molecules. Several hydrogen-bonded models containing two molecules (2A, 2T, or A+T), three molecules (3A, 3T, 2A+T, or 2T+A), or four molecules (4A, 4T, 3A+T, 3T+A, or 2A+2T) (see Supporting Information SP2) have been calculated. A comparison of the calculated structures with the STM images reveals, however, that a model consisting of 2A+2T molecules can best explain the cyclic substructures and additionally is the most appropriate model to attach to the single chains separating the cyclic substructure (see Supporting Information SP3). On the basis of the contrast in the STM image in Figure 2B, this binding feature can be observed between the cyclic substructures and the adjacent single chains.

When pure A and pure T molecules are dissolved individually in 1-octanol solutions, the individual base molecules tend to bind with each other, and dimer formation is predominant in each case, that is, A−A and T−T homodimers are formed, respectively. However, after mixing the two bases together, a "mixed phase" where there is a balance between homodimer formation versus heterodimer formation (i.e., A−A and T−T versus A−T dimers, respectively) is formed.

Binding between DNA complementary bases occurs mainly through Watson−Crick base pairing.[5] However, other alternative binding mechanisms between complementary DNA bases, such as reverse Watson−Crick, Hoogsteen, and reverse Hoogsteen base pairing, respectively, exist.[18] The Hoogsteen sites on purines, for example, play an important role in the tertiary structure of tRNAs,[19,20] for "wobble" codon−anticodon interactions,[21] and in DNA mispairing[22] and are also crucial in the formation of DNA triplexes.[23,24]

In SCC-DFTB calculations, we find that the binding energy of an A−A dimer is 0.468 eV/dimer (indicated with number 1 in Figures 3A and 4), which increases to 0.80 or 0.82 eV/dimer inside a molecular network for A−A homochiral chains (including two molecules per unit cell) or heterochiral chains (including four molecules per unit cell), respectively (see Supporting Information SP1). For the T−T dimer, we find a binding energy of 0.69 eV/dimer (indicated with number 2 in Figures 3A and 4), which increases to 0.74 eV/dimer inside the chain structure (Figure 1D).

Upon mixing A and T molecules together, we calculated four different possibilities of A−T heterodimers (indicated with numbers 3−6 in Figures 3A and 4).

Note that the binding energies of the complementary A−T heterodimers are very close to each other, and therefore, it is possible that all the A−T heterodimers presented in Figure 3A might be included in the mixed phase upon adsorption on the graphite surface.

The binding energies between the A−T heterodimers are found to be less than those of the homodimers (as reported recently).[25] However, the binding energies between the A−T heterodimers increase significantly when two A−T dimers approach each other to form a quartet that is impeded inside a molecular network, as revealed by the calculations shown in Figures 3B and 4, respectively.

The resulting network might be determined by the kinetics such that those dimers formed in the beginning lead to the preferred formation of dimers of the same kind to allow the formation of an energetically favorable network.

The four presented models of the A−T heterodimers (shown in Figure 3A) were consequently used to construct four kinds of A−T−A−T quartets, as illustrated in Figure 3B. From the SCC-DFTB calculations, we determined the binding energies of the different A−T−A−T quartets. As shown in Figure 4, the Hoogsteen A−T−A−T quartets (1.24 eV/quartet) and reverse Hoogsteen A−T−A−T quartets (1.20 eV/quartet) have significantly higher binding energies than Watson−Crick A−T−A−T quartets (0.8 and 1.08 eV/quartet) and reverse Watson−Crick A−T−A−T quartets (0.81 and 1.12 eV/quartet), respectively.

By comparing the supramolecular structures formed by the individual bases in the control experiments and in the A+T mixture, it is obvious that no quartet cyclic structures were observed under the present conditions in the control experiment of the pure A base molecules only. In addition, the calculations show that when four A molecules approach each other, A−A dimer formation is preferred, and when an A−A dimer binds to another A−A dimer, the orientation of the A−A dimers is altered from one row to another as shown in Figure 1A, leading to the formation of a complete A molecular network, without the formation of A quartet cyclic substructures.

Similarly, no T quartet cyclic substructures are observed in the control experiment when only pure T base molecules are observed. The calculations again show that T−T dimer formation is preferred with respect to the T quartet cyclic substructures.

However, when two mixed A−T heterodimers approach each other, binding occurs between the A−T heterodimers, leading to the formation of "a quartet" with a size similar to that of the cyclic structure observed in the STM images in Figure 2 and to the unit cell parameters (Table 1), respectively.

Due to the mixing molar ratio (350A:1T) used in the experiments, significantly more A molecules than T molecules are present in the mixed solution. Thus, it is not surprising that

(18) Hoogsteen, K. *Acta Crystallogr.* **1959**, *12*, 822−823.
(19) Robertus, J. D.; Ladner, J. E.; Finch, J. T.; Rhodes, D.; Brown, R. S.; Clark, B. F. C.; Klug, A. *Nature* **1974**, *250*, 546−551.
(20) Kim, S. H.; Suddath, F. L.; Qugley, G. J.; McPherson, A.; Sussman, J. L.; Wang, A. M. J.; Seeman, N. C.; Rich, A. *Science* **1974**, *185*, 435−440.
(21) Crick, F. H. C. *J. Mol. Biol.* **1966**, *19*, 548−555.
(22) Topal, M. D.; Fresco, J. R. *Nature* **1976**, *263*, 285−289.
(23) Moser, H. E.; Dervan, P. B. *Science* **1987**, *238*, 645−650.
(24) Francois, J. C.; Saison-Behmoaras, T.; Helene, C. *Nucleic Acids Res.* **1988**, *16*, 11431−11440.
(25) Kelly, R. E. A.; Kantorovich, L. N. *J. Mater. Chem.* **2006**, *16*, 1894−1905.

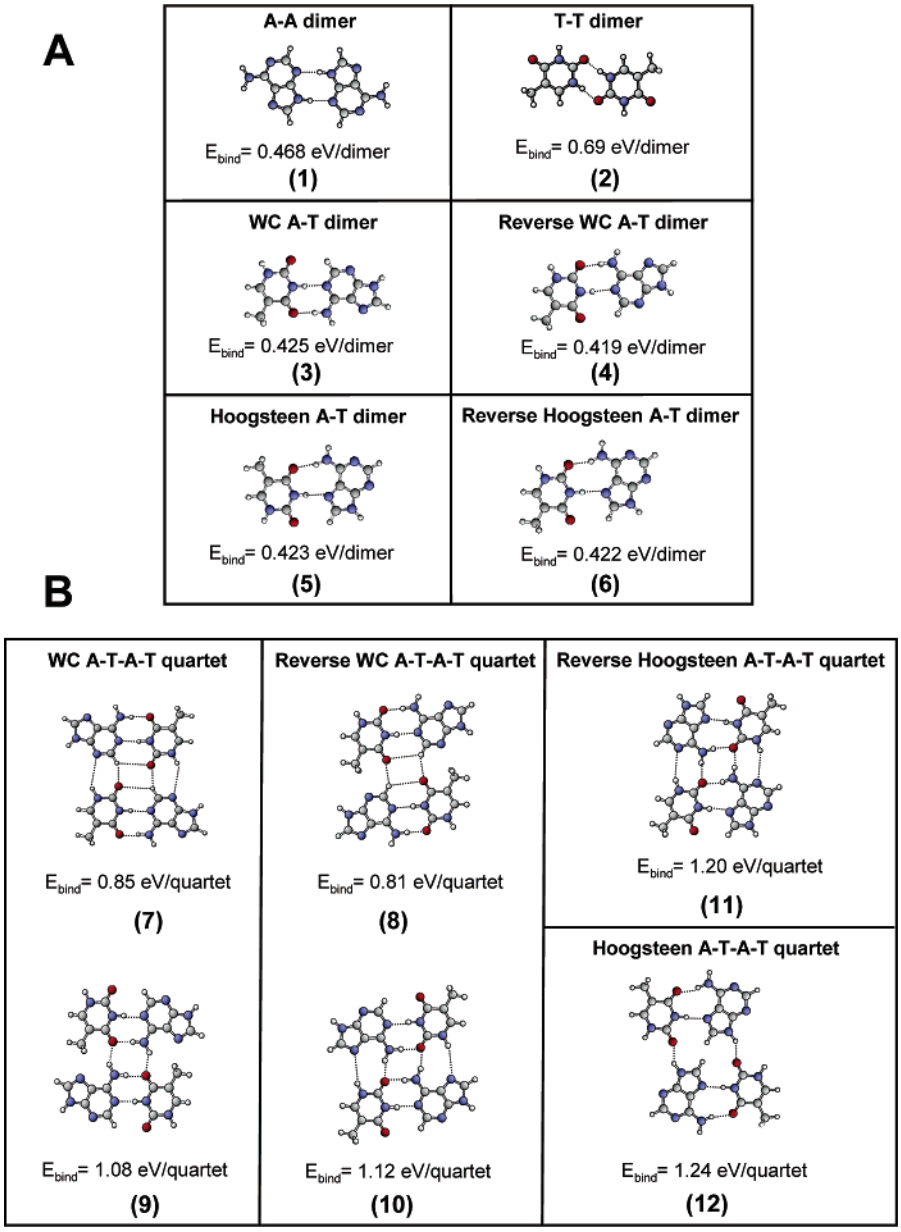

Figure 3. (A) A−A, T−T homodimers, and A−T heterodimers. (B) A−T−A−T quartets and their calculated binding energies. Numbers are used to differentiate between the A−A, T−T, and A−T dimers and the A−T−A−T quartets, which are also used in Figure 4. (For more proposed quartet models, see also Supporting Information SP2.)

several domains that contain only molecular networks formed by A−A dimers (data not shown) are observed, whereas the T molecules are mainly involved in the formation of A−T−A−T quartets.

Since there is an excess of A molecules present in the mixed solution, we therefore suggest that the single chains separating the A−T−A−T quartets observed in Figure 2 are composed of A−A dimers.

To identify which quartet of the proposed models presented in Figure 3B (and also in SP2) is more suitable for building up a molecular network that is similar to the STM image shown in Figure 2, all individual quartet models in addition to a single chain of A−A dimers were therefore superimposed on the STM image. In all calculated models except the reverse Hoogsteen A−T−A−T quartet model, when two quartets approach each other along unit cell vector *a*, the two quartets overlap with each other, and no binding occurs between the quartets along unit cell vector *a* and between the quartets and the A−A dimers chain along unit cell vector *b* (see Supporting Information SP2 and SP3).

Therefore, among all proposed models investigated for the combined quartet cycles and the single-chain structures, reverse Hoogsteen A−T−A−T quartets separated by homochiral chains of A−A dimers (Figure 2C) represent the best model. This specific model shows the best outcomes with respect to the contrast of the STM image, the size and shape of the quartet cycles and the single chains, the binding energies between the quartets, and the binding with the homochiral chains constructed by A−A dimers. The presence of the A−A dimers chains separating the quartets helps anchoring the A−T−A−T quartets' cycles via hydrogen bonding to stabilize the complete molecular network as depicted in Figure 2C.

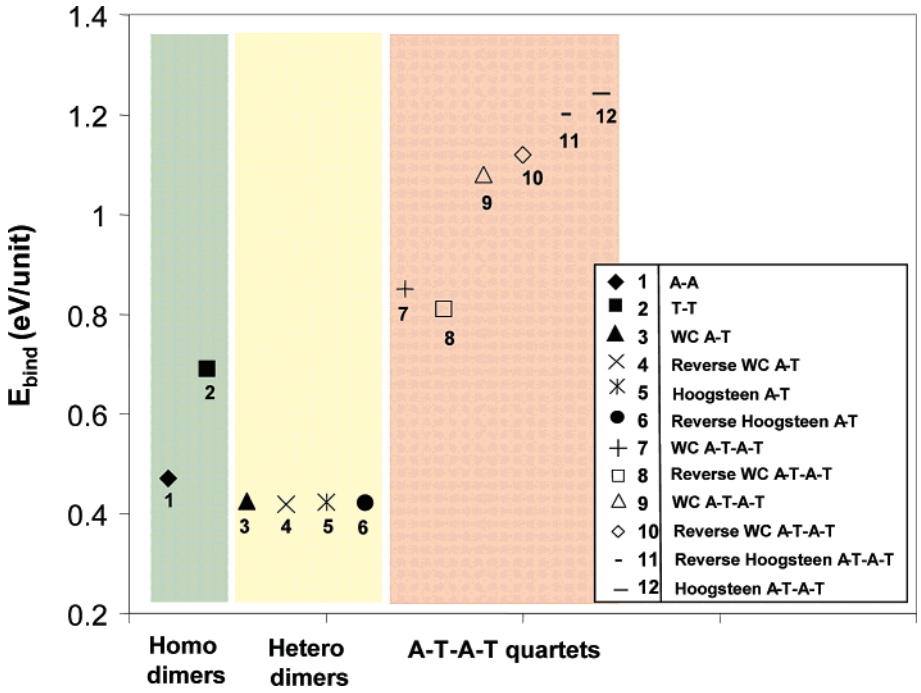

Figure 4. Binding energies of the homodimers (green plot), heterodimers (yellow plot), and A−T−A−T quartets (pink plot). The color code is only used for display purposes.

Moreover, there are more hydrogen bonds between the quartets and the adjacent A−A dimers chains and between the quartets along unit cell vector *a*; (i.e., three hydrogen bonds on each side of the quartet to the adjacent A−A chains plus two hydrogen bonds on each side of the quartet to the next quartets along unit cell vector *a*) (see Supporting Information SP3). Therefore, this model appears to be the most stable overall molecular network structure with a binding energy of 2.03 eV (per one A−T−A−T quartet and one A−A dimer in the unit cell).

The unit cell of the A−T−A−T quartets and the A−A homochiral chains, which includes six molecule, is determined, on the basis of the analysis of the STM images, to be $a = 1.0 \pm 0.2$ nm, $b = 2.3 \pm 0.2$ nm, and $\gamma = 88 \pm 2°$. Lattice parameters for the observed different adlayers structures of A, T, and the mixture A+T are summarized in Table 1.

The reverse Hoogsteen A−T−A−T quartets shown in Figure 2C appear as complete cyclic, or "doughnut", structures that are separated by small dark gap regions along unit cell vector *a*. This difference in contrast is related to the electron delocalization and the local density of states (LDOS)[26,27] in the quartet cycles and between two quartet cycles along unit cell vector *a*, respectively. Therefore, the high tunneling current observed in the quartet cycles suggests higher electron density of states between the molecular entities involved in the formation of these quartet cycles. On the other hand, the lower tunneling current detected in the dark gap regions indicates lower electron density of states.

This point is confirmed by the calculated model presented in Figure 2C showing that the binding energies inside the reverse Hoogsteen A−T−A−T quartets, illustrated with red rectangles, are around 1.2 eV/quartet, whereas the binding energy between two quartets along unit cell vector *a* is only 0.49 eV/quartet. These values were obtained using the structure of the molecular network without further relaxation. Furthermore, the number of hydrogen bonds differs in each case: eight hydrogen bonds exist inside a reverse Hoogsteen A−T−A−T quartet as illustrated in Figure 2C (between every two A and two T molecules), whereas the number of hydrogen bonds is reduced to only two between two reverse Hoogsteen A−T−A−T quartets along unit cell vector *a*, respectively.

4. Conclusions

In conclusion, we have presented novel 2D supramolecular nanostructures formed by DNA complementary bases on surfaces. When mixing A and T DNA bases, exquisite self-assembled nanoscale patterned structures consisting of quartet cyclic structures separated by single chains of dimers structures appeared. Theoretical SCC-DFTB calculations were carried out to obtain further insight into the observed structures, and from an interplay of the experimental and theoretical results, we propose a model consisting of reverse Hoogsteen A−T−A−T quartets separated by homochiral chains of A−A dimers that are stabilized by hydrogen bonding, leading to an overall stabilization of a molecular network. This model seems to fit all the features observed in the STM images. The cyclic features formed by the A+T mixture are related to similar structures, the so-called "quadruplexes" that consist of only one type of DNA bases, or a mixture of complementary DNA bases that have been found in biological processes through replication, transcription, and recombination[28] to telomere function. The novelty of this work is the formation of well-ordered A−T−A−T quartets, which offers new opportunities for host−guest complexation based on DNA bases. Furthermore, it might be useful for targeting new drugs that can be used in drug design and for targeting biological molecules. A natural extension of

(26) Lang, N. D. *Phys. Rev. Lett.* **1985**, *55*, 230−233.
(27) Gimzewski, J. K.; Möller, R. *Phys. Rev. B* **1987**, *36*, 1284−1287.
(28) Arthanari, H.; Bolton, P. H. *Chem. Biol.* **2001**, *8*, 221−230.

this work includes measuring the time scale of the stability of the observed phases at this molar ratio. In addition, mixing of complementary and noncomplementary DNA bases with different mixing molar ratios adsorbed on different substrates and also under variable temperatures creates nanopatterned surfaces with a high degree of complexity and functionalization.

Acknowledgment. We acknowledge financial support from the Danish Ministry for Science, Technology and Innovation through the iNANO Center from the Danish Research Councils. Computational resources were obtained from the Danish Center for Scientific Computing. E.R. thanks the Alexander von Humboldt Foundation for partial financial support in the form of a Feodor Lynen fellowship. We thank Ross Kelly and Dr. Lev Kantorovich for fruitful discussions.

Supporting Information Available: SP1 represents SCC-DFTB calculations of A−A dimers in homochiral and heterochiral chains. SP2 shows other possible quartets and their binding energies. SP3 illustrates a comparison between possible molecular networks that can be built up on the basis of all possible quartets presented in Figure 3B and in SP2. This material is available free of charge via the Internet at http://pubs.acs.org.

JA064988U